Global optimisation and growth simulation of AuCu clusters

T. J. Toai, G. Rossi and R. Ferrando*

Received 23rd May 2007, Accepted 21st June 2007
First published as an Advance Article on the web 14th September 2007
DOI: 10.1039/b707813g

Global optimisation techniques and Molecular Dynamics simulations are employed to investigate the structure and the chemical order of AuCu clusters, with composition $Au_{0.75}Cu_{0.25}$, $Au_{0.5}Cu_{0.5}$ and $Au_{0.25}Cu_{0.75}$. Global optimisations by Parallel Excitable Walkers algorithm have located the global minimum configurations of clusters at size $N = 100$, 160 and 200 atoms. Stable clusters do not exhibit any alloy-like ordering, and combine the tendency to surface segregation of the gold atoms with the icosahedral structural motif. As unique exception to the icosahedral trend, an almost perfect decahedron is located at size $N = 100$, exhibiting copper atoms in its outer shell. As regards to the dynamics, the paper deals with the growth of AuCu clusters, both depositing gold and copper atoms onto an heterogeneous seed, and depositing copper atoms onto an homogeneous gold seed. In agreement with the global optimisation results, the former growth process leads to the formation of Ih clusters, whose surface is enriched in gold atoms. The latter deposition process turns into the formation of decahedral clusters with a reversed $Cu_{shell}Au_{core}$ chemical ordering.

1. Introduction

The AuCu system has three bulk ordered alloys, $Au_{0.5}Cu_{0.5}$ (fcc, $L1_0$) $Au_{0.25}Cu_{0.75}$ and $Au_{0.75}Cu_{0.25}$ (fcc, $L1_2$). The alloy stoichiometries are quite well experimentally reproduced in clusters, both when the particles are synthesized by simultaneous reduction methods[1,2] and when they are produced by laser vaporization sources like that used by Pauwels *et al.*[3] In these experiments, optical, electron diffraction and HREM observations have been used to obtain information about the structural characteristics of the AuCu clusters dispersed in the colloidal solution, deposited on a carbon-coated grid and then dried[1] or deposited on MgO and amorphous carbon.[3] Pal and coworkers suggest a $Au_{shell}Cu_{core}$ arrangement, but focus essentially on the influence of composition on the structural distribution of the particles in the size-range 2–10 nm. On the other hand, the qualitative picture coming from the measurements by Pauwels is that the interaction with MgO forces the system to adopt a solid solution with fcc ordering, while several alternative packings are possible on the other, less interactive substrate. These findings confirm that AuCu is indeed quite a ductile system. This characteristic, together with the interest raised by gold nanoparticles in a variety of research fields, make AuCu an interesting object of investigation. In this paper we address the comparison between the AuCu structural configurations coming from global optimisation and growth simulations. The size

Dipartimento di Fisica, Università di Genova, Via Dodecaneso 33, 16136 Genova, Italy. E-mail: ferrando@fisica.unige.it

range considered is $30 < N < 300$. As entropic and kinetic effects can influence the growth pattern of clusters,[4,5] it is expected that the structural distributions coming from growth could not coincide with those coming from global optimisations. In particular, we will focus on the fitness of core-shell chemical ordering as varying size and composition, and on the competition between decahedral and icosahedral structural motifs.

2. Model, method and simulation plan

2.1 Potential function

The potential used to model the atomic interactions was proposed by Cleri and Rosato.[6] It is a semi-empirical potential derived within the tight-binding second-moment approximation. Cluster potential energy E is given by the sum over all the atoms of their bonding and repulsive energy:

$$E = \sum_j (E_j^{\mathrm{b}} + E_j^{\mathrm{r}}) \tag{1}$$

Where the bonding term E_j^{b} is expressed as:

$$E_j^{\mathrm{b}} = -\sqrt{\sum_i \xi_{sw}^2 \mathrm{e}^{\left[-2q_{sw}\left(\frac{r_{ji}}{r_{sw}^0}-1\right)\right]}} \tag{2}$$

The repulsive Born–Mayer term E_j^{r} is:

$$E_j^{\mathrm{r}} = \sum_i A_{sw} \mathrm{e}^{\left[-p_{sw}\left(\frac{r_{ji}}{r_{sw}^0}-1\right)\right]} \tag{3}$$

r_{ij} is the distance between the atoms at sites *i.e.* j; s = A, B is the chemical species of the atom j, while w = A, B is the species of the atom i. r_{sw}^0 is the nearest-neighbours distance. If $s = w$, it coincides with the pure metal *nn* distance. If the interaction is heteroatomic, *i.e.* $s \neq w$, r_{sw} is expressed as:

$$r_{\mathrm{AB}}^0 = r_{\mathrm{BA}}^0 = \frac{r_{\mathrm{AA}}^0 + r_{\mathrm{BB}}^0}{2} \tag{4}$$

The parameters A_{sw}, p_{sw}, q_{sw}, ξ_{sw} are fitted to several bulk properties of the $Au_{0.25}Cu_{0.75}$ cubic alloy. The potential is able to predict with accuracy the occurrence of the structural order–disorder transition in the alloy. A cut-off analytical function is used from the Au fifth-neighbours distance on.

2.2 Global optimisation method

Small AuCu clusters ($N < 30$) have been studied by means of a genetic[7,8] global optimization approach by Lordeiro *et al.*[9] This size limit was extended up to 45 atoms by Rapallo *et al.*[10] Here a Parallel Excitable Walkers (PEW)[11] algorithm is used as an efficient tool to deal with the global optimisation of heterogeneous clusters of larger sizes. The algorithm performs parallel Basin Hopping searches.[12,13] Each walker explores a different region of a geometric order parameter space, and the information about the low-energy clusters belonging to such different geometrical basins is retained during the optimisation. In the code-setup used to optimise the AuCu clusters, minima have been classified according to the percentage of local fivefold symmetries in the cluster. Clusters have been optimised at size N = 100, N = 160 and N = 200, considering all the three alloy stoichiometries.

Our optimisation procedure consists of two parts. First, for each size and composition we run 8 PEW simulations of 5×10^5 steps. In these simulations, the *shake* move is employed. In the shake move, each atom of the cluster is displaced

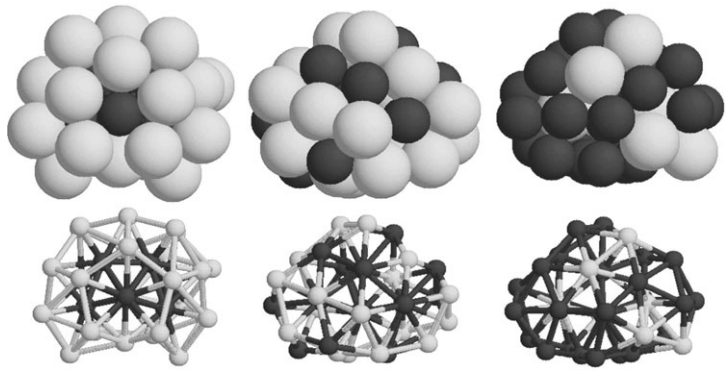

Fig. 1 The 34-atom seeds of the growth simulations, which correspond to global minima located by a basin hopping procedure for the compositions $Au_{26}Cu_8$, $Au_{17}Cu_{17}$ and Au_8Cu_{26}. Dark and light atoms represent, respectively copper and gold atoms.

randomly within a sphere of radius 1.3 Å, centered around its present position. We have verified that this kind of move is the most efficient in exploring different geometric structures. We classify the results of these simulations according to the percentage of (5,5,5) Common Neighbours Analysis signatures. In this way, we are able to build up a database of structures belonging to different geometrical motifs. For the best structures of each motif, we run Basin Hopping simulations in which only the *exchange* moves are employed. In such a kind of move, two atoms of different species are swapped. These exchange runs are made at low temperature in order to optimize chemical ordering in the clusters.

2.3 Growth simulation method

Growth simulations are performed by Molecular Dynamics simulations. Newton equations are implemented by a Velocity Verlet algorithm with a time step $\tau = 7 \times 10^{-15}$ s. Temperature is controlled by means of an Andersen Thermostat, and atoms are deposited one by one with a delay of $\tau_{dep} = 7 \times 10^{-9}$ s.

Two sets of growth simulations have been performed. The simulations of the first set reproduce the growth of clusters with the three alloy stoichiometries. Simulations start from a 34-atom seed whose composition is Au_8Cu_{26}, $Au_{17}Cu_{17}$, $Au_{26}Cu_8$, respectively (see Fig. 1). When an atom has to be deposited, a random number is extracted in order to give the atom its chemical species, according to the desired composition. Growth simulations take place at two temperatures, $T = 400$ K and $T = 500$ K. For each composition and temperature, three independent simulations are performed. Simulations stop at size $N = 200$ atoms. The second set of simulations starts from an homogeneous icosahedral gold core of 147 atoms. Copper atoms are then deposited onto the seed, up to size $N = 310$ atoms. This allows us to make some comparisons between the structure and the chemical order of clusters with $Au_{0.5}Cu_{0.5}$ composition which are grown by two different deposition processes.

3. Results

3.1 Global optimisation results

3.1.1 A Homogeneous clusters. The global optimisation of homogeneous Au and Cu clusters at size $N = 100$, $N = 160$ and $N = 200$ has been performed first. The results are summarized in Table 1. At the smallest size, gold and copper have quite a different behaviour, gold preferring to adopt an fcc ordering and copper favouring the icosahedral configurations. It is worth noting that homogeneous Cu minima based on the icosahedral motif can have both a Mackay (Ih-M) and an anti-Mackay

Table 1 Global minima for homogeneous Au and Cu clusters, and heterogeneous $Au_{0.25}Cu_{0.75}$, $Au_{0.5}Cu_{0.5}$, $Au_{0.75}Cu_{0.25}$

Composition	$N = 100$	$N = 160$	$N = 200$
Au	Fcc	Fcc	Dh
Cu	Ih-M	Ih-aM	Dh
$Au_{0.25}Cu_{0.75}$	Dh	Ih-aM	Ih-M
$Au_{0.5}Cu_{0.5}$	Ih-M	Ih-aM	Ih-M
$Au_{0.75}Cu_{0.25}$	double Ih	Ih-aM	Ih-M

(Ih-aM) external layer. At size $N = 200$, the decahedral motif is favoured by both the metals, even if in the case of copper there is a strict competition between the Dh and the Ih-M motif.

3.1.1 B $Au_{0.75}Cu_{0.25}$. As a general characteristic of the mixed composition clusters, one can notice that the icosahedral motif is preferred to the decahedral one. Darby *et al.*[14] demonstrated that the introduction of a single copper impurity into a homogeneous Au_{55} cluster can shift its global minimum structure from the amorphous to the icosahedral basin. According to the global optimisations, at size $N = 100$, $N = 160$ and $N = 200$ the gold-rich clusters adopt different Ih-based structures. The one-hundred atom cluster is a double icosahedron, containing two interpenetrating Ih_{55} and a small anti-Mackay patch (see Fig. 2). Both the Ih_{55} have a copper atom in their central site, then there is a mixed gold and copper layer constituting the surface of both the Ih_{13}, and finally the surface is composed by gold atoms only. This can thus be considered a three-shell configuration. At size $N = 160$, the global minimum cluster is a Ih_{147} partially covered by an anti-Mackay shell. The cluster has again a gold surface. Finally, at size $N = 200$ the global optimisation procedure has located a Mackay icosahedron (Ih_{147} plus a Mackay patch). It is worth noting that this structure is in close competition with the icosahedron covered by the anti-Mackay patch, differing by less than 0.12 eV. The $L1_2$ alloy ordering in the bulk is thus not reproduced at these small sizes. This finding is somehow a validation of the model, since Yasuda and Mori[15] found by TEM observations that solid solution becomes more stable than the ordered $L1_2$ low-temperature phase even at room temperature when the cluster diameter is reduced below approximately 5 nm. The location of stable $Au_{shell}Cu_{core}$ particles is coherent also with other previous findings of Ascencio *et al.*[2]

3.1.1 C $Au_{0.5}Cu_{0.5}$. All the three sizes analysed present an icosahedral global minimum. The perfect Ih_{55} and Ih_{147} are covered by an external Mackay shell at size $N = 100$ and $N = 200$, while at the intermediate size $N = 160$ the anti-Mackay

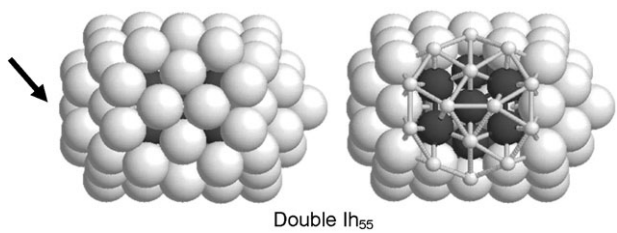

Fig. 2 The double icosahedron which is the global minimum structure for $Au_{0.75}Cu_{0.25}$ at size $N = 100$ (dark atoms represent copper, light atoms represent gold). One of the Ih_{55} misses a vertex atom, as indicated by the arrow on the left. The double Ih is partially covered by an anti-Mackay patch, indicated by the small atoms on the right.

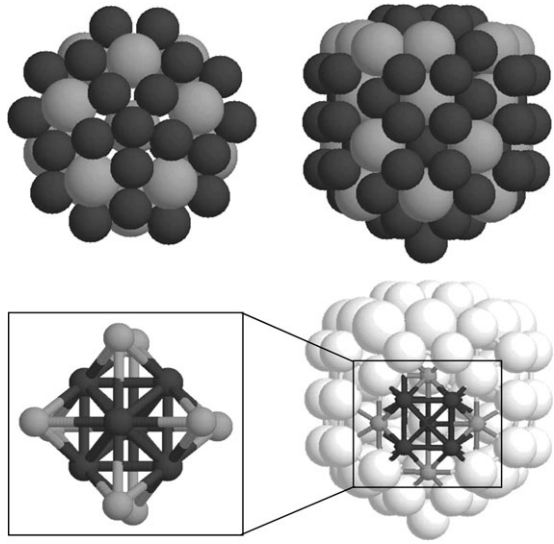

Fig. 3 The Dh $Au_{25}Cu_{75}$ global minimum cluster. In the first row, a top and side view of the structure. Dark and light atoms represent, respectively copper and gold. In the second row, the right snapshot highlights the position of a fragment of a unit cell of the $L1_2$ alloy within the decahedral arrangement.

patch is preferred to the Mackay one. Even at this intermediate composition there is a tendency to form core-shell structures.

3.1.1 D $Au_{0.25}Cu_{0.75}$. The picture is somehow different at the copper-rich composition. At size $N = 100$, the global minimum structure is indeed a decahedron, namely the perfect Marks Dh_{101} missing a vertex atom. This Dh accommodates gold and copper atoms so as to reproduce the chemical order of the $L1_2$ bulk alloy (see Fig. 3). In such a structure, the core-shell order is reversed, and the copper atoms are positioned on the external (100) facets of the cluster (the radial distribution of the cluster is depicted in Fig. 4). The exception of a Dh global minimum structure is due to the combination of a geometrical and a chemical driving force. The former is the

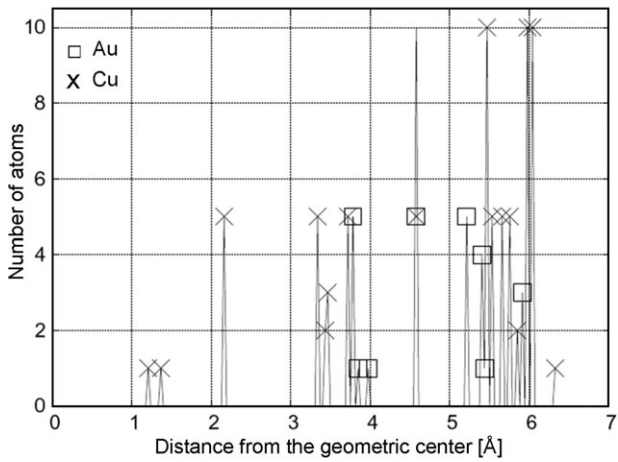

Fig. 4 The radial distribution of atoms in the global minimum of the cluster $Au_{25}Cu_{75}$. Cu atoms occupy the external (100) facets.

presence of a magic size for the decahedral motif, and the latter is the possibility to accommodate the $L1_2$ chemical order into each tetrahedron of the Dh. At size $N = 160$ the anti-Mackay patch covers the Ih_{147}, in the same way as for the other stoichiometries. The Mackay stacking is the lowest energy one at size $N = 200$.

3.2 Growth results

The results of the growth simulations are summarized in Table 2. All the clusters grown from an heterogeneous 34-atom seed follow an icosahedral pattern, so that at size $N = 200$ their structure is made of a Ih_{147} core, plus an external, incomplete icosahedral patch. This outer layer can exhibit either a Mackay or an anti-Mackay pattern (see Fig. 5). The smallest amount of copper in the cluster ($Cu_{0.25}Au_{0.75}$) is

Table 2 Structure and chemical order of the 200-atom clusters resulting from the growth simulations upon a 34-atom seed. From the left: temperature of the growth simulations, final structure of the cluster at size $N = 200$, number of Cu atoms in the cluster, percentage of Au atoms on the surface, percentages of homogeneous and heterogeneous nearest-neighbours bonds

$Au_{0.75}Cu_{0.25}$	Structure	Cu atoms	% of Au on surf.	% Au–Au	%Cu–Cu	%Au–Cu
$T = 400$ K						
1	Ih_{147} + M patch	53	92	49	10	41
2	Ih_{147} + M patch	46	95	54	9	37
3	Ih_{147} + aM patch	60	90	44	15	41
$T = 500$ K						
1	distorted Ih	49	92	52	8	40
2	Ih_{55} + M patch	56	98	45	13	42
3	distorted pIh	51	96	51	38	11

$Au_{0.25}Cu_{0.75}$						
$T = 400$ K						
1	Ih_{147} + aM patch	157	21	4	59	37
2	Ih_{147} + M patch	141	32	7	50	43
3	Ih_{147} + M patch	140	32	8	49	43
$T = 500$ K						
1	Ih_{147} + M patch	145	33	6	54	40
2	Ih_{147} + M patch	144	36	6	54	40
3	Ih_{147} + M patch	151	28	5	59	36

$Au_{0.5}Cu_{0.5}$						
$T = 400$ K						
1	Ih_{147} + M patch	106	59	19	30	51
2	Ih_{147} + aM patch	99	60	22	26	52
3	Ih_{147} + aM patch	94	66	24	26	50
$T = 500$ K						
1	Ih_{147} + aM patch	99	66	21	29	50
2	Ih_{147} + M patch	92	75	25	29	46
3	Ih_{147} + M patch	109	58	19	34	47

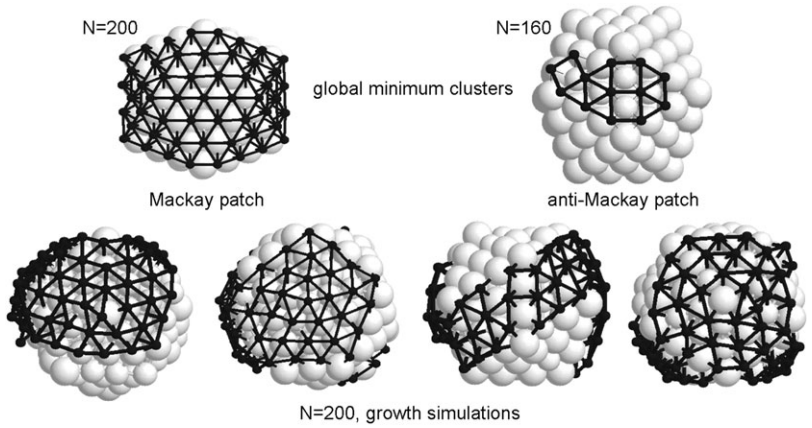

Fig. 5 Icosahedral clusters with Mackay (left) and anti-Mackay (right) patches. The atoms of the patches are dark and smaller, regardless of their species. In the top row, the Mackay and anti-Mackay global minimum clusters at size $N = 200$ and $N = 160$ for the $Au_{0.75}Cu_{0.25}$ composition. In the bottom row, on the left, two examples of clusters grown with a Mackay patch upon the Ih_{47} core. On the right, two examples of anti-Mackay patches.

thus sufficient to boost the formation of icosahedral structures during the growth process. In such icosahedral clusters, regardless of the composition, some segregation of gold to the surface of the cluster can be observed. As reported in Table 2, the percentage of Au atoms on the surface almost always exceeds the gold concentration in the whole cluster. Nevertheless, clusters are not perfectly core–shell. The Ih_{13} core of the clusters is never composed by Cu atoms only. Also in $Cu_{0.75}Au_{0.25}$ clusters, the central Ih_{13} has at least one gold atom in its 12-atom shell. The chemical order of the clusters is thus characterized by a copper-rich core, a mixed intermediate shell, and a gold-rich external shell. This shows that AuCu clusters can assume a three-shell arrangement. This arrangement is however different from the one obtained in simulations of AgCu and AgNi growth (where there was no intrashell intermixing) but it has a striking resemblance to the three-shell pattern experimentally observed in AuPd.[16]

A different scenario arises when the growth of the cluster is simulated starting from an homogeneous Au core and depositing Cu atoms upon it. It has been proved that in other heterogeneous metallic systems, the deposition of A atoms onto a seed of B atoms can determine the formation of core-shell[17] or three-shell onion-like clusters.[18] We thus analysed the growth of an Au icosahedral core of 147 atoms up to 310 atoms ($Au_{147}Cu_{163}$). The choice of an icosahedral seed, despite the fact that homogeneous gold does not exhibit an icosahedral arrangement in this size range, has two main reasons. First of all, the icosahedral motif should become the most favorable as soon as a few copper atoms approach the cluster, coherently with the results of global optimisations. Moreover, the icosahedral structure could favour the effects[19,20] of fast-alloying, encouraging the small copper atoms to incorporate to the core of the cluster and help to release some volume strain.

At the end of the 6 growth simulations, both at $T = 400$ K and $T = 500$ K, five clusters have a decahedral morphology, and one is ordered according to an fcc structure with stacking fault. In order to locate the size at which the Ih $\rightarrow$ Dh transition takes place, one can perform a local minimisation of the snapshots collected during growth, and estimate the stability of each configuration by the Δ index, defined as:

$$\Delta_N = \frac{E - 147E_{coh}^{Au} - NE_{coh}^{Cu}}{N^{2/3}} \quad (5)$$

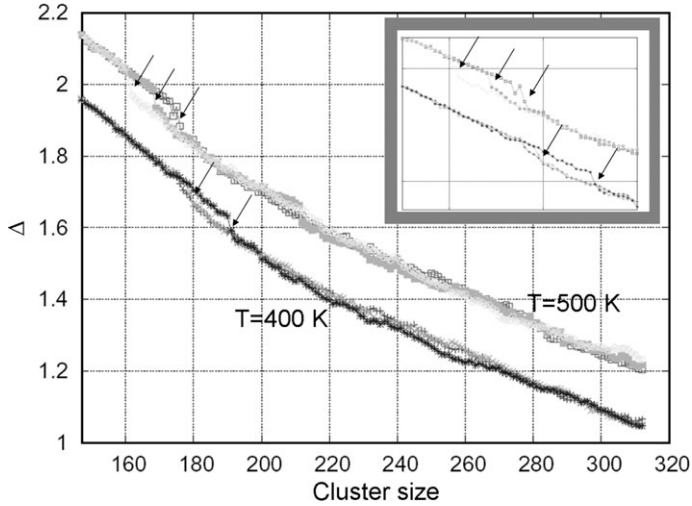

Fig. 6 Δ values referred to the snapshots collected through the simulation of the deposition of Cu atoms on a Au_{147} icosahedral core.

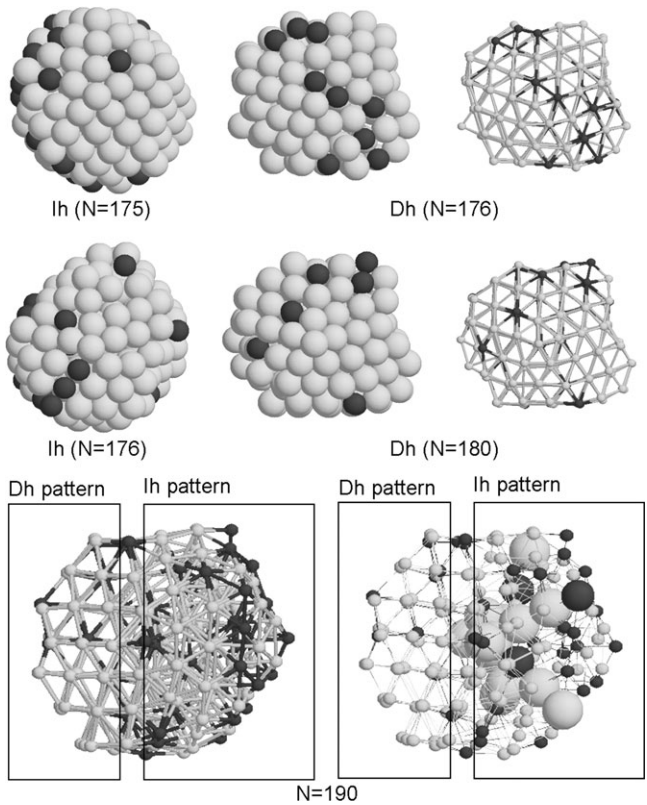

Fig. 7 Snapshots from the simulation of the growth of Cu atoms on an Au_{147} icosahedral core. Simulations have been led at $T = 400$ K. In the first and second row, the transition from the icosahedral motif (on the left) to the decahedral one (right) in two independent growth simulations. On the bottom, a snapshot from a growth simulation showing a cluster which is transforming from Ih to Dh. The right snapshot shows in space fill representations the atoms belonging to the fivefold axis of the incomplete icosahedron.

Low Δ values refer to stable structures. The denominator is introduced to compensate the scaling of Δ with the size of the cluster, while the drift observed in Fig. 6 is due to the increase of the more cohesive atoms, Cu, in the cluster. Drops in the Δ curves refer to the structural transition from the icosahedral to the decahedral motif. Please note that, in this size range, the icosahedral-like skeletal structure has the lower energy, as predicted by global optimisation. The stability of the icosahedral motif is nevertheless strictly related to the chemical order of the cluster, and it is well accomplished only by the partial core–shell ordering previously described. Our simulation proves that, in the timescale of the simulated growth upon a Au_{147} core, copper atoms have neither the energy nor the time needed to incorporate the gold surface, and the decahedral arrangement becomes preferred to the icosahedral one. In Fig. 7 some snapshots coming from the simulations at $T = 400$ K are shown. It is worth noting that the existence of $Au_{core}Cu_{shell}$ decahedra has been previously postulated by Ascencio *et al.*,[2] who recognized that during the synthesis of bimetallic colloidal AuCu particles different configurations can coexist in the sample, and not in all the cases do the clusters exhibit their lowest energy structure and chemical order. Molecular Dynamics simulation of the heating of such decahedral particles proved that the chemical order of the particle is reversed before melting, so as to achieve the more stable $Au_{shell}Cu_{core}$ configuration.

4. Conclusions

In this paper both global optimisation techniques and Molecular Dynamics simulations are used to study the structure and the chemical order of AuCu nanoclusters. The sizes considered extended up to 200 atoms for the global optimisation study, and up to 300 atoms for the clusters resulting from growth simulations.

The picture arising from the search for the lowest-energy configurations is characterized by the prevalence of the icosahedral motif, that is typical of homogeneous copper clusters and is instead quite unusual for homogeneous gold clusters at equilibrium.[21] Icosahedral structures are characterized by the tendency of gold to segregate at the surface of the cluster. At the compositions $Au_{0.5}Cu_{0.5}$ and $Au_{0.25}Cu_{0.75}$ the segregation is not complete, and clusters with some gold atoms in the core are found as global minimum configurations.

The structural and chemical analysis of the clusters resulting from the growth simulations of AuCu clusters, by deposition onto an heterogeneous 34-atom seed, confirms the tendency to build up icosahedral clusters. It is likely to observe both anti-Mackay and Mackay patches over cluster surfaces, and such patches are usually enriched in gold atoms. Following the suggestion coming from some previous experimental studies,[22] the deposition of Cu atoms onto a gold core of 147 atoms has been simulated. Despite the fact that a small amount of copper should lead to the formation of icosahedral and partially core–shell structures, at the growth temperature of 400 and 500 K no incorporation of the copper atoms into the core has been observed. The cluster indeed transforms from Ih to Dh before getting to the size $N = 200$. This again confirms the output of the global optimisations, as the Dh structure located at size $N = 100$ and composition $Au_{0.25}Cu_{0.75}$ exhibits Cu atoms in its outer sites. In the decahedral structure, copper atoms can find a better surface arrangement than in the icosahedral structure, where surface bonds are quite stretched. Moreover, in the decahedral geometries there is no driving force causing Cu atoms to reach the cluster center fast, at variance with the case of icosahedral clusters.

References

1 U. Pal, J. F. Sanchez Ramirez, H. B. Liu, A. Medina and J. A. Ascencio, *Appl. Phys. A*, 2004, **79**, 79.
2 J. A. Ascencio, H. B. Liu, U. Pal, A. Medina and Z. L. Wang, *Microsc. Res. Tech.*, 2006, **69**, 522.

3 B. Pauwels, G. Van Tendeloo, E. Zhurkin, M. Hou, G. Verschoren, L. Theil Khun, W. Bouwen and P. Lievens, *Phys. Rev. B*, 2001, **63**, 165406.
4 F. Baletto, C. Mottet and R. Ferrando, *Phys. Rev. Lett.*, 2000, **84**, 5544.
5 F. Baletto, C. Mottet and R. Ferrando, *Phys. Rev. B*, 2001, **63**, 155408.
6 F. Cleri and V. Rosato, *Phys. Rev. B*, 1993, **48**, 22.
7 R. L Johnston, *Dalton Trans.*, 2003, **22**, 4193.
8 N. T. Wilson and R. L. Johnston, *J. Mater. Chem.*, 2002, **12**, 2913.
9 R. A. Lordeiro, F. F. Guimarães, J. C. Belchior and R. L. Johnston, *Int. J. Quantum Chem.*, 2003, **95**, 112.
10 A. Rapallo, G. Rossi, R. Ferrando, A. Fortunelli, B. C. Curley, L. D. Lloyd, G. M. Tarbuck and R. L. Johnston, *J. Chem. Phys.*, 2005, **122**, 194308.
11 G. Rossi and R. Ferrando, *Chem. Phys. Lett.*, 2006, **423**, 17.
12 D. J. Wales and J. P. K. Doye, *J. Phys. Chem.*, 1997, **28**, 5111.
13 D. J. Wales, *Energy Landscapes*, Cambridge University Press, Cambridge, 2003.
14 S. Darby, T. V. Mortimer Jones, R. L. Johnston and C. Roberts, *J. Chem. Phys.*, 2002, **116**, 1536.
15 H. Yasuda and H. Mori, *Z. Phys. D*, 1996, **37**, 181.
16 D. Fevrer, A. Torres-Castro, X. Gao, S. Sepulveda-Guzman, U. Ortiz-Mendez and M. J. Yacaman, *Nano Lett.*, in press.
17 F. Baletto, C. Mottet and R. Ferrando, *Phys. Rev. B*, 2002, **66**, 155420.
18 F. Baletto, C. Mottet and R. Ferrando, *Phys. Rev. Lett.*, 2003, **90**, 135504.
19 H. Yasuda, H. Mori, M. Komatsu, K. Takeda and H. Fujita, *J. Electron Microsc.*, 1992, **41**, 267.
20 H. Mori, H. Yasuda and T. Kamino, *Philos. Mag. Lett.*, 1994, **69**, 279.
21 K. Koga and K. Sugawara, *Surf. Sci.*, 2003, **529**, 23.
22 H. Yasuda and H. Mori, *Z. Phys. D*, 1994, **31**, 131.

